Developmental Cell, Vol. 1, 363–375, September, 2001, Copyright ©2001 by Cell Press

zyg-8, a Gene Required for Spindle Positioning in *C. elegans*, Encodes a Doublecortin-Related Kinase that Promotes Microtubule Assembly

Pierre Gönczy,[1,4,5] Jean-Michel Bellanger,[1,5] Matthew Kirkham,[2] Andrei Pozniakowski,[2] Karine Baumer,[1] Jennifer B. Phillips,[3] and Anthony A. Hyman[2]

[1]Swiss Institute for Experimental Cancer Research (ISREC)
CH-1066 Lausanne
Switzerland

[2]Max-Planck-Institute for Molecular Cell Biology and Genetics
D-01307 Dresden
Germany

[3]Institute of Molecular Biology
University of Oregon
Eugene, Oregon 97403

Summary

Proper spindle positioning is essential for spatial control of cell division. Here, we show that *zyg-8* plays a key role in spindle positioning during asymmetric division of one-cell stage *C. elegans* embryos by promoting microtubule assembly during anaphase. ZYG-8 harbors a kinase domain and a domain related to Doublecortin, a microtubule-associated protein (MAP) affected in patients with neuronal migration disorders. Sequencing of *zyg-8* mutant alleles demonstrates that both domains are essential for function. ZYG-8 binds to microtubules in vitro, colocalizes with microtubules in vivo, and promotes stabilization of microtubules to drug or cold depolymerization in COS-7 cells. Our findings demonstrate that ZYG-8 is a MAP crucial for proper spindle positioning in *C. elegans*, and indicate that the function of the Doublecortin domain in modulating microtubule dynamics is conserved across metazoan evolution.

Introduction

Asymmetric divisions are central to the generation of cell fate diversity. During development, asymmetric divisions often give rise to daughter cells that differ not only in fate, but also in size. For such divisions to occur in animal cells, the mitotic spindle must be asymmetrically localized by the end of anaphase, when the cleavage furrow is specified to bisect the mitotic spindle (reviewed in Rappaport, 1971).

Microtubules play an important role in spindle positioning in many organisms. Thus, an intact microtubule cytoskeleton is required for proper positioning of the spindle in *Drosophila* neuroblasts or in budding yeast (Kaltschmidt et al., 2000; Knoblich et al., 1995; Palmer et al., 1992). Recent evidence in *S. cerevisiae* indicates that the mechanisms underlying proper spindle positioning include selective stabilization of microtubules through interaction between Bim1p present at the plus end of microtubules and the cortical anchor Kar9p (Korinek et al., 2000; Lee et al., 2000; Miller et al., 2000). Comparatively little is known in metazoans about the mechanisms that regulate microtubule behavior to ensure proper spindle positioning.

We chose to address this question in the one-cell stage *C. elegans* embryo, where spindle position can be observed with high spatial and temporal resolution using time-lapse differential interference contrast (DIC) microscopy. In wild-type, the spindle sets up in the cell center but moves slightly toward the posterior during anaphase, leading to an asymmetric spindle position along the anteroposterior (AP) axis. This results in the unequal cleavage of the one-cell stage embryo into a larger anterior blastomere and a smaller posterior one. Spindle positioning during anaphase occurs in response to AP polarity cues established earlier in the cell cycle by six maternally required *par* genes and an atypical PKC (Kemphues et al., 1988; Tabuse et al., 1998; reviewed in Kemphues and Strome, 1997). In embryos lacking one of these components, polarity along the AP axis is altered; probably as a consequence, posterior spindle displacement usually does not take place, and the first division is symmetric. Several PAR proteins have a polarized distribution along the AP axis in one-cell stage embryos. Thus, the PDZ-containing proteins PAR-3 and PAR-6 both localize to the anterior cortex (Etemad-Moghadam et al., 1995; Hung and Kemphues, 1999). Conversely, PAR-2, a ring finger-containing protein, and PAR-1, a Ser/Thr protein kinase, both localize to the posterior cortex (Boyd et al., 1996; Guo and Kemphues, 1995). Despite the wealth of information on components establishing polarity in this and other systems, little is known about how polarity is coordinated with modulation of cytoskeletal behavior to achieve accurate spindle position.

Here, we show that *zyg-8* is a key component directing spindle positioning in one-cell stage *C. elegans* embryos. In *zyg-8* mutants, the spindle moves in an exaggerated manner toward the posterior during anaphase. We establish that this results from a defect in microtubule assembly and that *zyg-8* encodes a Doublecortin-related kinase that protects microtubules against depolymerization. Our work reveals that stabilization of microtubules during anaphase is necessary for polarity to translate into appropriate asymmetric spindle positioning.

Results

zyg-8 Mutant Embryos Have Spindle Positioning Defects

We sought to identify loci essential for proper spindle positioning in one-cell stage *C. elegans* embryos. In wild-type, spindle positioning follows from two processes. First, the two centrosomes and associated pronuclei move to the cell center while undergoing a 90° rotation. As a result, the spindle sets up in the cell center and along the AP axis (Figure 1A, top). Second, during

[4]Correspondence: pierre.gonczy@isrec.unil.ch
[5]These authors contributed equally to this work.

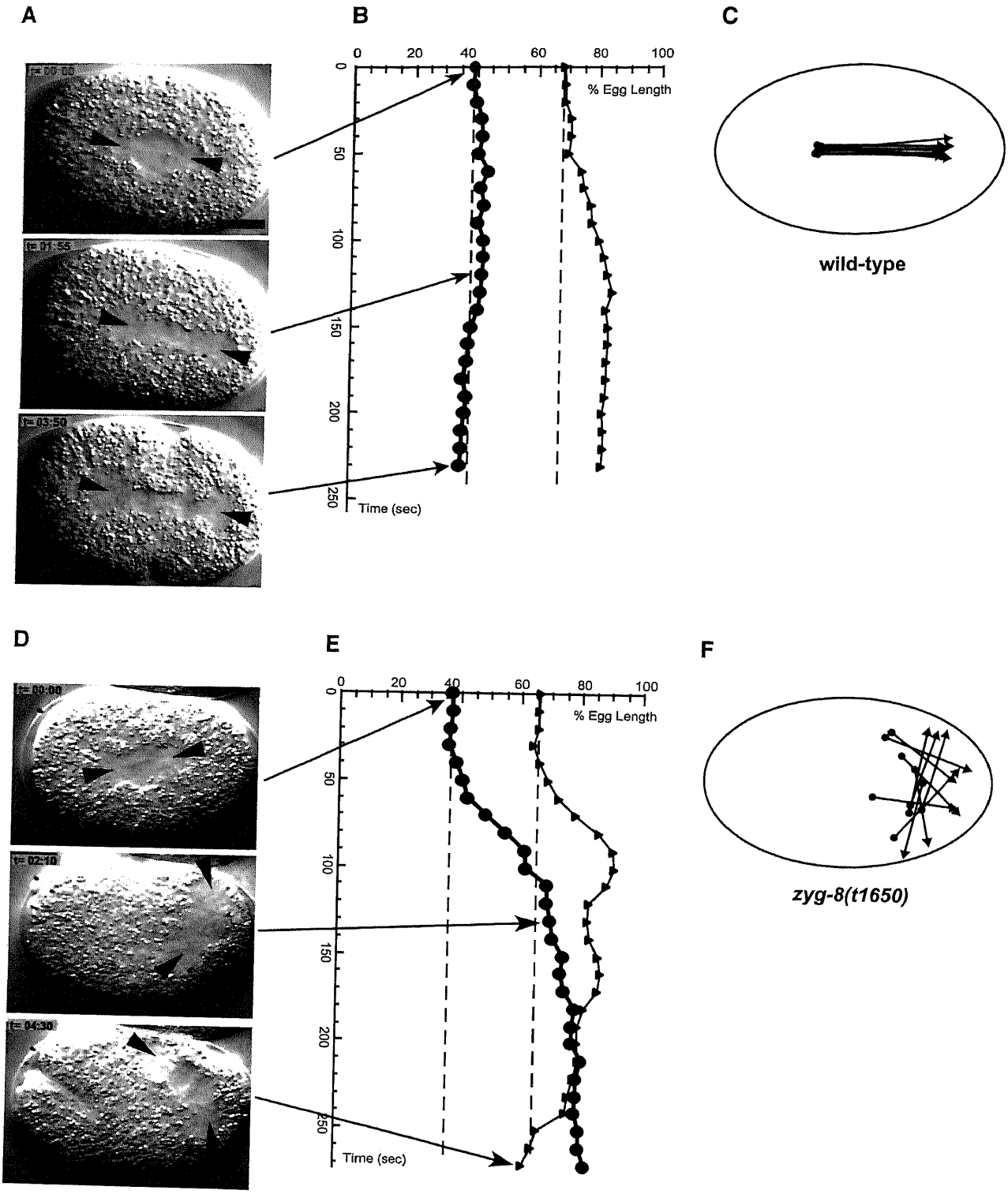

Figure 1. Anaphase Spindle Positioning Defects in *zyg-8* Mutant Embryos

Wild-type (A–C) and *zyg-8(t1650)* mutant (D–F) one-cell stage embryos. Anterior (0% egg-length) is to the left, posterior (100% egg-length) to the right in this and other figures.

(A and D) Time-lapse DIC microscopy recordings. Arrowheads point to the center of asters. Time elapsed since the beginning of the sequence is displayed in minutes and seconds. All panels are at same magnification. Bar = 10 μm.

(B and E) Tracings of aster position. Filled circles: anterior aster; triangles: posterior aster. Note that the spindle reorients perpendicular to the longitudinal axis after reaching the vicinity of the posterior cortex, most likely due to the lack of space.

(C and F) Schematic representation of spindle position at the end of mitosis in 10 embryos of each genotype. Filled circles: anterior aster; triangles: posterior aster. *zyg-8(t1650)* embryos in which rotation was between 45° and 90° are represented. Note that spindle length in *zyg-8(t1650)* embryos is less than in wild-type.

anaphase, the posterior spindle pole is displaced slightly toward the posterior (Figure 1A, middle; Figure 1B). As a result, the spindle is asymmetrically positioned along the AP axis, leading to unequal cleavage into a larger anterior blastomere and a smaller posterior one (Figure 1A, bottom; Figure 1C).

Table 1. Phenotypes of *zyg-8* Mutant Embryos

Genotype*	n	Two Female Pronuclei	Premature Rotation[a]	Spindle Position Defects	Rotation <45°; Average Angle[b]	Rotation ≥45°; Average Angle[c]
N2	25	0	0	0	3 (12%); 23°	22 (88%); 80°
zyg-8(t1650)	34	8 (24%)	5 (15%)[d]	34 (100%)	10 (29%); 16°	24 (71%); 76°
zyg-8(t1547)	23	1[e] (4%)	2 (9%)	23 (100%)	9 (39%); 25°	14 (61%); 70°
zyg-8(b235ts)	23	0	7 (30%)	23[f,g] (100%)	6 (26%); 20°	17 (74%); 74°
zyg-8(t1650)/tDf5	10	0[h]	1 (10%)	10 (100%)	2 (20%); 13°	8 (80%); 70°

Analysis by time-lapse DIC microscopy; angle of rotation scored just prior to breakdown of pronuclear envelopes; percentages and angles rounded off to the nearest integer. There were two additional phenotypes in some *zyg-8* mutant embryos: (1) a slight delay in female pronuclear formation, indicative of potential defects during female meiotic divisions; (2) the presence of two daughter nuclei reforming on either side of the aberrant cleavage furrow, indicative of potential defects in chromosome segregation.

*Relevant genotype of parents is given; animals were homozygous for the indicated genotype [except for *zyg-8(t1650)/tDf5*].

[a] In some embryos, rotation of centrosomes occurred prior to full migration of the female pronucleus, leading to the placement of the female pronucleus anterior of the spindle. As a result, only paternally contributed chromosomes were segregated by the spindle in these embryos.

[b] Average rotation angle in the subset of embryos in which rotation was less than 45°.

[c] Average rotation angle in the subset of embryos in which rotation was equal to or greater than 45°.

[d] Only 32 *zyg-8(t1650)* embryos were scoreable for the potential occurence of premature rotation.

[e] This embryo had three female pronuclei.

[f] In one *zyg-8(b235)* mutant embryo, rotation failed, and the spindle remained in the middle of the embryo, resulting in a symmetric division.

[g] In most *zyg-8(b235)* mutant embryos, the spindle was thin and often seemed to break in two during exaggerated posterior spindle movement.

[h] Occasional *zyg-8(t1650)/tDf5* in other experiments did harbor two female pronuclei.

We screened a collection of maternal-effect embryonic lethal mutations by time-lapse DIC microscopy and identified mutations in a locus called *zyg-8* (Wood et al., 1980) that result in dramatic spindle positioning defects in one-cell stage embryos (Gönczy et al., 1999). Spindle positioning was aberrant in all embryos derived from *zyg-8(t1650)* homozygous mutant hermaphrodites (hereafter referred to as *zyg-8* mutant embryos). In ~29% (10/34) *zyg-8* mutant embryos, rotation of the centrosomes was less than 45°, and the spindle set up transverse to the AP axis (Table 1). In most of these embryos (9/10), the spindle drifted toward the anterior or lateral cortex during anaphase. In ~71% (24/34) *zyg-8* mutant embryos, rotation was between 45° and 90°, and the spindle set up in the cell center and along the AP axis, like in wild-type (Table 1; Figure 1D, top). However, in the vast majority of these embryos (23/24), the spindle was displaced in a strikingly exaggerated manner toward the posterior during anaphase (Figure 1D, middle; Figures 1E and 1F). Movies of anaphase spindle positioning in wild-type and *zyg-8* mutant embryos can be viewed at http://www.embl-heidelberg.de/ExternalInfo/hyman/Data.htm.

We found similar spindle positioning defects in 7/9 nonconditional and 6/6 temperature-sensitive *zyg-8* alleles (Table 1 and Experimental Procedures). Importantly, these phenotypes were also observed in the progeny of animals transheterozygous for *zyg-8(t1650)* and *tDf5*, a deficiency uncovering the region to which *zyg-8* has been mapped genetically (Table 1). These findings provide strong evidence that spindle positioning defects result from a diminution in *zyg-8* function. While there were other less penetrant phenotypic manifestations in *zyg-8* mutant embryos (Table 1), these observations taken together indicate that *zyg-8* acts predominantly to restrict the extent of posterior spindle displacement during anaphase of one-cell stage *C. elegans* embryos.

Polarity Cues and Their Interpretation Are Not Abolished in *zyg-8* Mutant Embryos

Exaggerated posterior spindle displacement during anaphase could be due in principle to a primary defect in AP polarity cues. To test this hypothesis, we examined the distribution of four markers of polarity in *zyg-8* mutant embryos: PAR-3, PAR-2, PAR-1, and PGL-1, a P granule component (Kawasaki et al., 1998). We found that the distribution of all four markers was essentially indistinguishable from wild-type. PAR-3 protein was restricted to the anterior cortex (21/21 embryos; Figure 2B), PAR-2 and PAR-1 to the posterior cortex (22/22 and 22/23 embryos, respectively; Figures 2D and 2F), while P granules were segregated to the posterior (21/21 embryos; Figure 2H). These observations indicate that exaggerated posterior anaphase spindle displacement in *zyg*-8 mutant embryos does not result from defects in AP polarity.

We next investigated whether this phenotype was due to a lack in communicating polarity cues to the cytoskeleton. If communication was abolished, then spindle positioning in *zyg-8* mutant embryos should not be sensitive to changes in AP polarity. To test whether this was the case, we examined spindle positioning in *zyg-8* mutant embryos in which AP polarity was altered by removing *par-3*, *par-2*, or *par-1* function. We restricted our analysis to embryos in which the rotation was between 45° and 90°, as such embryos almost always undergo exaggerated posterior spindle displacement during anaphase in the absence of *zyg-8* function alone. We found that exaggerated posterior displacement no longer took place in most *zyg-8 par-3* double mutant embryos, as well as in *zyg-8* mutant embryos in which *par-2* or *par-1* function was silenced by RNAi; instead, the anaphase spindle was typically located toward the embryo center (Figures 2I–2K). These observations demonstrate that *zyg-8* mutant embryos respond to changes in AP polarity, indicating that communication between polarity cues and the cytoskeleton is not abolished in the absence of *zyg-8* function.

Defects in Anaphase Microtubule Assembly Likely Cause the *zyg-8* Mutant Phenotype

We next investigated whether the *zyg-8* mutant phenotype may result from defects in the microtubule cytoskeleton. We found that microtubules in *zyg-8* mutant

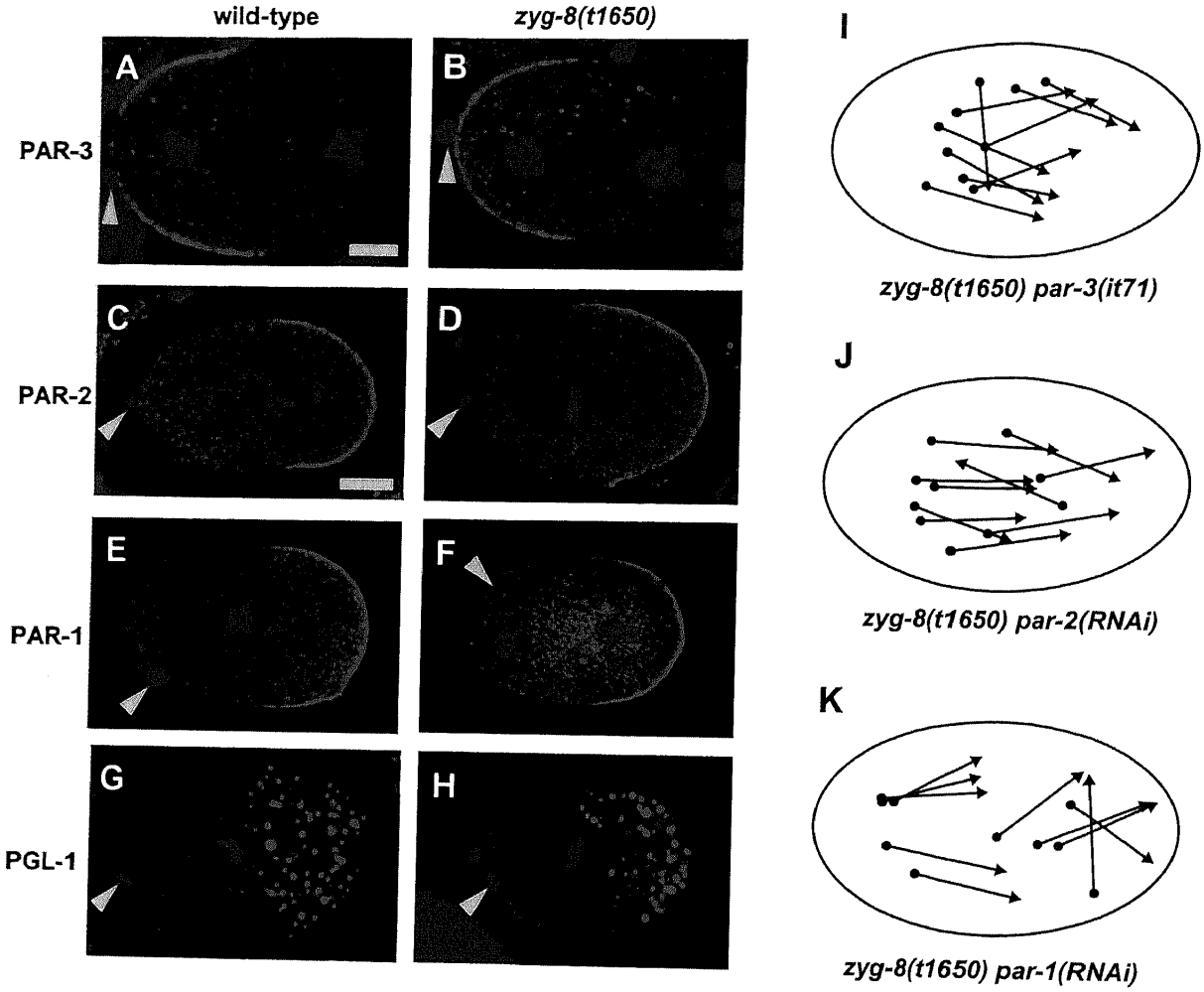

Figure 2. Polarity Cues and Their Interpretation Are Not Affected in *zyg-8* Mutant Embryos

Wild-type (A, C, E, and G) and *zyg-8(t1650)* mutant (B, D, F, and H) one-cell stage embryos stained with anti-PAR-3 (A and B), anti-PAR-2 (C and D), anti-PAR-1 (E and F), and anti-PGL-1 (G and H) antibodies (all shown in red) and counterstained with Hoechst 33258 to reveal DNA (shown in blue). (A) and (B), as well as (C)–(H), are at same magnification. Bars = 10 μm. Arrowheads point to polar body material.

(A and B) Cortical PAR-3 is restricted to the anterior; both embryos are at early pronuclear migration stage.

(C and D) Cortical PAR-2 is restricted to the posterior; embryo in (C) is at pronuclear meeting, embryo in (D) at metaphase.

(E and F) Cortical PAR-1 is restricted to the posterior; embryo in (E) is just after pronuclear meeting, embryo in (F) at early pronuclear migration.

(G and H) P granules segregate to the posterior; both embryos are just before metaphase.

(I–K) Schematic representation of spindle position at the end of mitosis in 10 *zyg-8(t1650) par-3 (it71)* (I), *zyg-8(t1650) par-2(RNAi)* (J), and *zyg-8(t1650) par-1(RNAi)* (K) embryos. Whether the difference in spindle behavior apparent between removal of either *par-2* or *par-3* and that of *par-1* is significant remains to be determined with a larger data set.

embryos were essentially indistinguishable from wild-type prior to anaphase (Figures 3A and 3B, and data not shown). During anaphase, however, astral microtubules were markedly shorter than normal (Figures 3C and 3D). The longest astral microtubules projecting toward the anterior cortex were 17.4 μm on average in wild-type (SD = 0.8; n = 15), but only 13.0 μm (SD = 1.7; n = 15) in *zyg-8* mutant embryos. As a result, while many astral microtubules were in the immediate vicinity of the anterior cortex in wild-type, the longest astral microtubules were on average 3.4 μm (SD 1.4; n = 15) away from it in *zyg-8* mutant embryos. Astral microtubules projecting toward the posterior cortex were similarly shorter; in addition, spindle microtubules may be affected as well, since the spindle often appeared somewhat wider than in wild-type (see Figure 5E). Similar global alterations in anaphase microtubules were observed in two other *zyg-8* alleles (*t1518* and *t1547*).

While examining fixed specimens by indirect immunofluorescence microscopy, we noted that there was no significant anaphase B in *zyg-8* mutant embryos (Experimental Procedures). In wild-type, the average distance between the two spindle poles increased from 10.9 μm (SD = 0.8; n = 13) in metaphase to 15.2 μm (SD = 2.5; n = 13) in anaphase. In contrast, there was no increase in the average pole to pole distance between metaphase (11.7 μm; SD = 1.1; n = 11) and anaphase (11.5 μm; SD = 1.0; n = 22) in *zyg-8* mutant embryos. Nevertheless, sister chromatids always separated (see Figure 3D).

To address whether the observed alterations in anaphase microtubules were causing exaggerated posterior spindle displacement in *zyg-8* mutant embryos, we

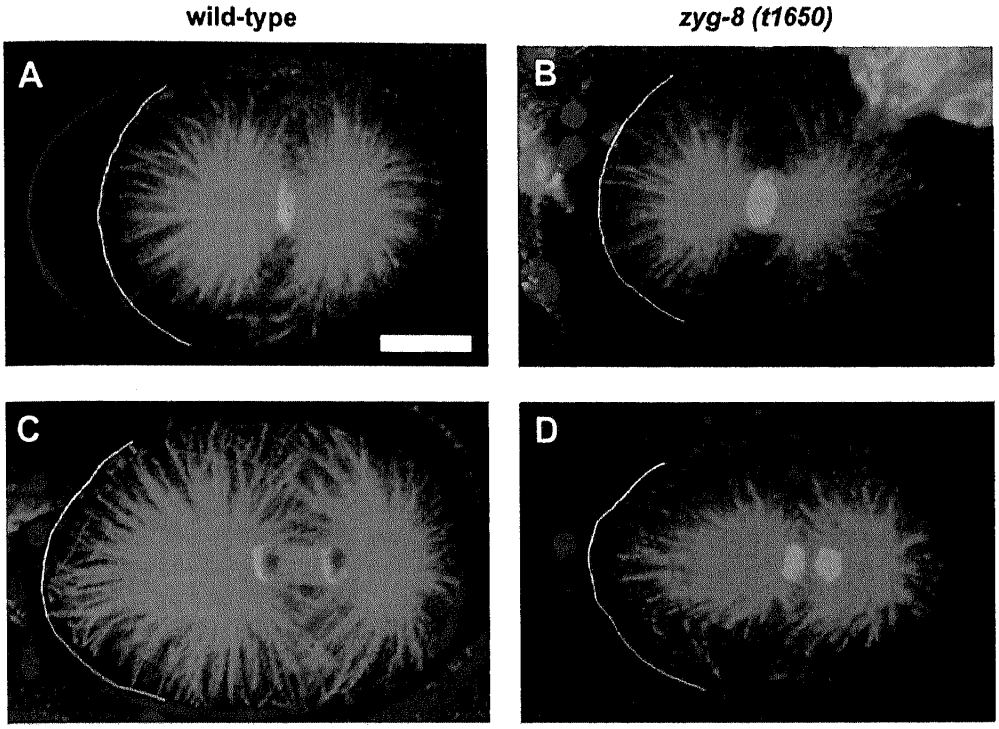

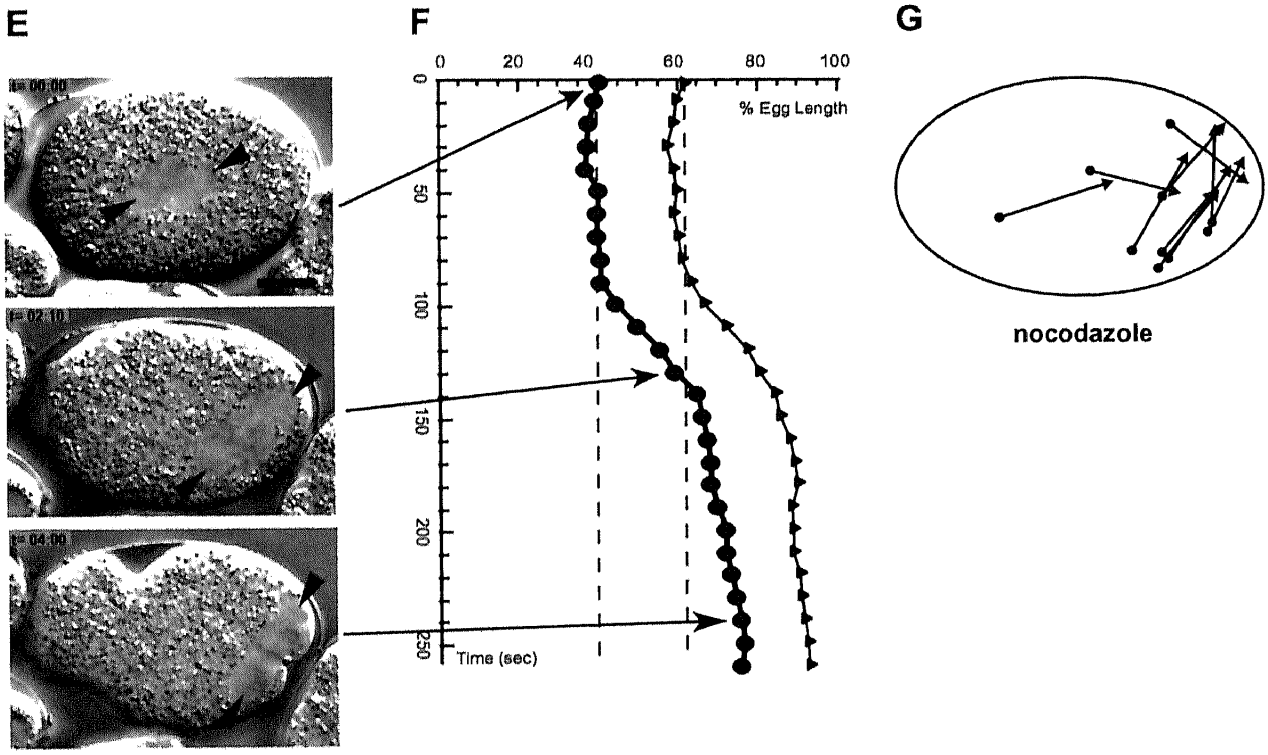

Figure 3. Defects in Anaphase Microtubule Assembly Likely Cause the *zyg-8* Mutant Phenotype

(A–D) Wild-type (A and C) and *zyg-8(t1650)* mutant (B and D) one-cell stage embryos stained with anti-tubulin antibodies (shown in green) and counterstained with Hoechst 33258 to reveal DNA (shown in blue). (A and B) Metaphase. (C and D) Anaphase. All panels approximately at same magnification. Bar = 10 μm. White contour: anterior-most cortex. Note that astral microtubules during anaphase are shorter in the *zyg-8* mutant embryo and do not extend all the way to the cortex. Although this particular *zyg-8* mutant embryo is slightly smaller than wild-type, similar alterations in the microtubule network were observed in *zyg-8* mutant embryos of normal size.

(E–G) Time-lapse DIC microscopy recording (E), tracings of aster position (F), and schematic representation of spindle position at the end of mitosis in 10 wild-type embryos treated with nocodazole during anaphase (G). Bar = 10 μm; symbols are as in Figure 1.

asked whether this phenotype could be generated by subjecting wild-type anaphase embryos to the microtubule-destabilizing agent nocodazole. We found this to be the case for 14/15 embryos tested (Figures 3E–3G). Therefore, shorter/less stable microtubules during anaphase indeed cause excess posterior spindle displacement and likely explain the *zyg-8* mutant phenotype.

In summary, our phenotypic analysis indicates that

A

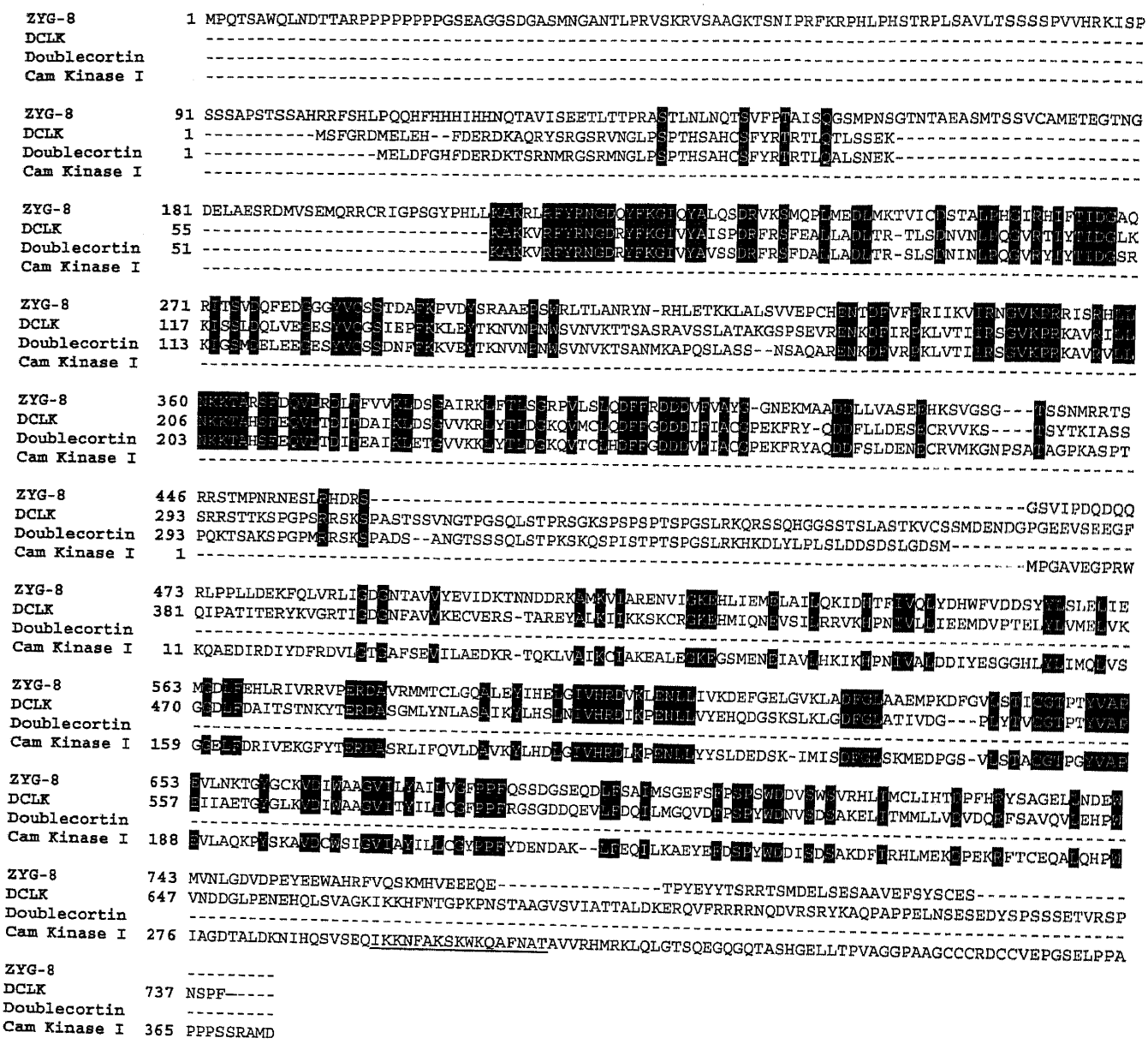

B

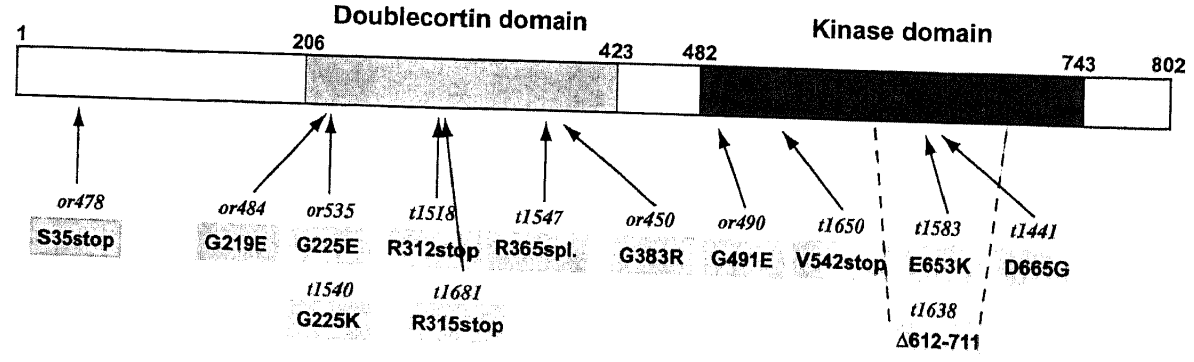

Figure 4. Predicted ZYG-8 Protein

(A) Comparison between predicted protein sequences of ZYG-8 (802 aa), human DCLK (740 aa), human Doublecortin (360 aa), and rat Cam kinase I (374 aa), aligned using ClustalW 1.81. Residues identical in three of the proteins are highlighted. The Ca/Cam binding domain of Cam kinase I is underlined (Picciotto et al., 1993).

zyg-8 function normally promotes microtubule assembly during anaphase, ensuring proper spindle positioning and asymmetric cell division.

zyg-8 Encodes a Doublecortin-Related Kinase

We sought to identify the molecular nature of *zyg-8*. We found that injection of dsRNA corresponding to a candidate ORF in the interval to which *zyg-8* had been mapped genetically yielded progeny with a *zyg-8* like phenotype (Gönczy et al., 2000). Two corresponding partial cDNAs were sequenced, and RT-PCR utilized to obtain the 5′ end of the transcript, which is predicted to encode an 802 aa protein (Figure 4A). We sequenced this gene in *zyg-8* mutant alleles, which led to the identification of four nonsense mutations that result in stop codons in the predicted protein sequence at positions 35, 312, 315, and 542, respectively, and of a mutation in a splice donor consensus sequence that is predicted to result in a truncated protein (Figure 4B). Surprisingly, the *zyg-8* allele that results in a stop codon at position 35 is temperature sensitive. While it remains to be elucidated why this allele retains function at the permissive temperature, these observations taken together provide compelling evidence that this gene corresponds to the *zyg-8* locus.

Homology searches revealed that ZYG-8 has orthologs in other metazoans and harbors two notable protein domains (Figures 4A and 4B). First, ZYG-8 contains a domain similar to human Doublecortin (DCX; 48% aa identity over 215 aa). The doublecortin gene is mutated in patients with X-linked lissencephaly and double-cortex syndrome and encodes a MAP that stimulates microtubule polymerization in vitro (des Portes et al., 1998; Francis et al., 1999; Gleeson et al., 1998; Gleeson et al., 1999; Horesh et al., 1999). Second, ZYG-8 contains a kinase domain similar to calcium/calmodulin kinases (41% aa identity over 260 aa with rat CaM kinase I). Sequencing of additional *zyg-8* alleles revealed that both Doublecortin and kinase domains are essential for *zyg-8* function (Figure 4B). Four alleles have single aa substitutions in conserved residues of the Doublecortin domain, including one (G383 in ZYG-8) that is mutated in an X-linked lissencephaly pedigree (Sapir et al., 2000; Taylor et al., 2000). One allele is missing a substantial portion of the kinase domain, while three alleles have single aa substitutions in conserved residues of the kinase domain. One of these (G491 in ZYG-8) is conserved in all protein kinases and essential for ATP binding, while another (D665 in ZYG-8) is nearly invariantly conserved and crucial for stabilizing the catalytic loop (Hanks and Hunter, 1995).

ZYG-8 Is a Microtubule-Associated Protein

We next addressed whether ZYG-8 is a MAP. We first tested whether ZYG-8 binds to microtubules in vitro. ^{35}S-labeled ZYG-8 was generated in reticulocyte lysate and added to increasing amounts of taxol-stabilized microtubules. ZYG-8 bound to microtubules was separated from unbound ZYG-8 by sedimentation through a glycerol cushion; following SDS/PAGE, the pellet and supernatant fractions were quantitated by autoradiography and densitometry. After correcting for the small amount of ZYG-8 pelleted in the absence of microtubules, we found that ~30% ZYG-8 cosediments with 10 μM microtubules (Figure 5A).

We next generated a ZYG-8::GFP fusion protein to examine ZYG-8 distribution in living embryos. The fusion construct rescued the maternal-effect embryonic lethality of two *zyg-8* mutant alleles (Experimental Procedures), indicating that GFP distribution likely reflects that of endogenous ZYG-8. Using dual time-lapse DIC and fluorescence spinning disc confocal microscopy, we determined that ZYG-8::GFP concentrates in areas of high microtubule density, such as the spindle and spindle poles during mitosis (Figures 5B and 5C). In addition, ZYG-8::GFP is present at low levels in the cytoplasm throughout the cell cycle and detectable at centrosomes during prophase (Figure 5C and data not shown). Colocalization of ZYG-8 with microtubules was confirmed by indirect immunofluorescence microscopy with antibodies raised against ZYG-8 (Figures 5D and 5F). This aspect of the staining pattern reflects bona fide ZYG-8 distribution because it is absent in *zyg-8* mutant embryos (Figures 5E and 5G).

Taken together, these observations demonstrate that ZYG-8 behaves as a MAP both in vitro and in vivo.

ZYG-8 Colocalizes with Microtubules and Promotes Their Stability in Mammalian Cells through the Doublecortin Domain

We next wanted to ascertain which domain of ZYG-8 confers the ability to associate with microtubules. To this end, we first transfected HA-tagged full-length ZYG-8 into COS-7 cells. We found that HA-ZYG-8 colocalizes with microtubules (Figures 6A, 6D, and 6G). Similarly, the Doublecortin domain alone tagged with HA and transfected into COS-7 cells localizes to microtubules (Figures 6B, 6E, and 6H). In contrast, the kinase domain alone localizes to the cytoplasm (Figures 6C, 6F, and 6I). These results demonstrate that the Doublecortin domain of ZYG-8 is both necessary and sufficient for colocalization with microtubules. Compatible with this view, we found that HA-ZYG-8 carrying either of three single aa substitutions in the Doublecortin domain found in *zyg-8* alleles (*or484*, *or535*, *or450*) also fails to colocalize with microtubules in COS-7 cells (data not shown).

We then tested whether the presence of full-length ZYG-8 leads to protection of microtubules against depolymerization by drug or cold, as has been shown for other MAPs (Takemura et al., 1992). We found this to be the case indeed. Strikingly, over 95% of cells (n = 170) that had an extensive microtubule network despite the presence of 10 μM nocodazole expressed HA-ZYG-8

(B) ZYG-8 domain composition (SMART analysis) and alterations in mutant alleles. The mutation in *t1547* changes a consensus splice donor sequence between exons 2 and 3; this is predicted to result in the inclusion of intron 2 in the mRNA and the addition of 39 non-sense aa after exon 2, followed by a stop codon. The mutation in *t1638* results in the skipping of an exon encoding a portion of the kinase domain.

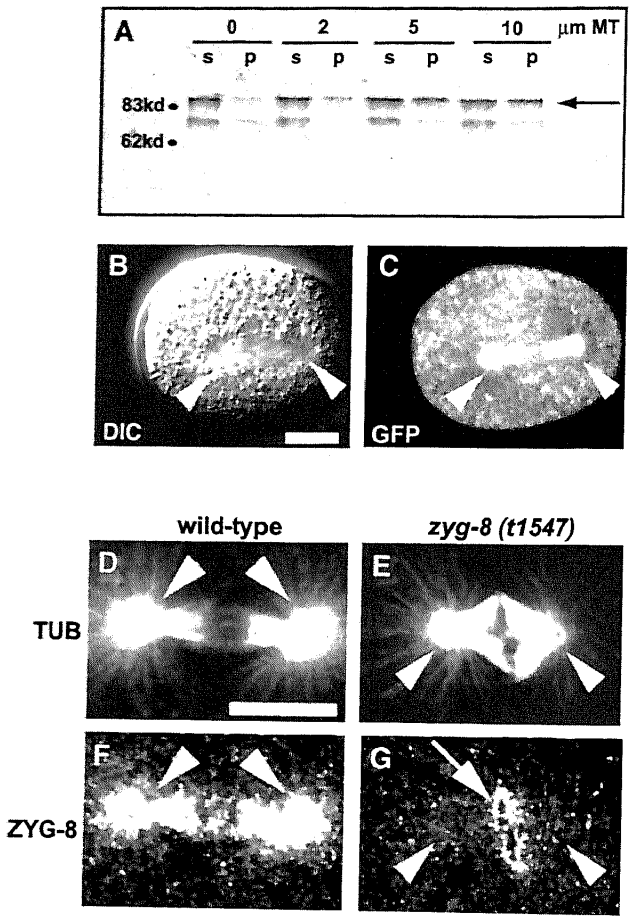

Figure 5. ZYG-8 Is a Microtubule-Associated Protein

(A) In vitro cosedimentation assay. ^{35}S-labeled ZYG-8 incubated with 0, 2, 5, or 10 μM taxol-stabilized microtubules (MT), spun, and separated on SDS-PAGE prior to autoradiography and densitometry. s, supernatant; p, pellet. Approximately 30.5% of ZYG-8 cosedimented with 10 μM microtubules in this experiment (average = 29%; SD = 7; n = 5 experiments). The principal translation product (arrow) has an apparent molecular weight of ~85 kDa – the expected size for full-length ZYG-8. The smaller species may result from internal translation initiation, premature chain termination or degradation of the full-length product.

(B and C) DIC (B) and fluorescence spinning disc confocal microscopy (C) of anaphase *zyg-8(t1650)* mutant embryo carrying GFP::ZYG-8. Bar ≈10 μm. GFP::ZYG-8 concentrates on the spindle and spindle poles (arrowheads) and is present at lower levels in the cytoplasm.

(D–G) Wild-type anaphase (D and F) and *zyg-8(t1547)* mutant metaphase (E and G) one-cell stage embryos stained with anti-tubulin (D and E) and anti-ZYG-8 (F and G) antibodies. (D)–(G) are at the same magnification. Bar = 10 μm. Anti-ZYG-8 antibodies mark the spindle and spindle poles (arrowheads) in wild-type. Note the somewhat thicker spindle in the *zyg-8* mutant embryo; note also that anti-ZYG-8 antibodies recognize an epitope on the nuclear envelope that is not specific to ZYG-8 (G, arrow). Similar results were obtained with *zyg-8(t1518)* and *zyg-8(t1650)*.

(Figures 6J, 6M, and 6P). Similarly, 100% of cells (n = 170) that had a robust microtubule array after cold treatment expressed the construct. Stabilization of microtubules was achieved in the presence of the Doublecortin domain alone (Figures 6K, 6N, and 6Q). In contrast, transfection of the kinase domain alone offered no protection against microtubule disassembly (Figures 6L, 6O, and 6R). Therefore, ZYG-8 activity promotes microtubule stability through the Doublecortin domain.

Discussion

zyg-8 Is Required Primarily during Anaphase to Promote Microtubule Assembly

Our phenotypic analysis suggests that *zyg-8* promotes microtubule assembly primarily during anaphase, when the most penetrant phenotype is observed in mutant embryos: exaggerated posterior-directed spindle displacement. Importantly, this phenotype is distinct from that observed in embryos lacking *zyg-9* function (Albertson, 1984). ZYG-9 is homologous to XMAP215, a major regulator of microtubule dynamics in *Xenopus* egg extracts (Gard and Kirschner, 1987; Matthews et al., 1998; Tournebize et al., 2000). In *zyg-9* mutant embryos, microtubules are shorter than normal throughout the cell cycle. As a consequence, microtubule-dependent processes that normally occur early in the first cell cycle, such as pronuclear migration, fail to take place. In contrast, pronuclear migration is not affected in *zyg-8* mutant embryos.

There are other less penetrant phenotypes in *zyg-8* mutant embryos. Occasionally, formation of the female pronucleus is delayed, and multiple female pronuclei are present (see Table 1), suggesting that *zyg-8* plays some role during the meiotic divisions, perhaps during anaphase. In addition, ~30% *zyg-8* mutant one-cell stage embryos fail to undergo rotation of the centrosomes, indicating a partial requirement of *zyg-8* just prior to mitosis, compatible with the fact that rotation is a microtubule-dependent process (Hyman and White, 1987). However, microtubules at that stage in *zyg-8* mutant embryos are indistinguishable from wild-type by indirect immunofluorescence microscopy. In contrast, during anaphase, microtubules in mutant embryos are markedly shorter than normal. These observations taken together suggest that *zyg-8* is required primarily during anaphase to promote microtubule assembly.

ZYG-8 and Temporal Control of Microtubule Dynamics

Microtubule dynamics change drastically during the cell cycle (reviewed in Desai and Mitchison, 1997). Dynamicity is low during interphase, resulting in long microtubules on average, and high during metaphase, resulting in short microtubules on average. Extensive microtubule elongation then takes place during anaphase, resulting again in longer microtubules and stabilization of the elongating spindle (Vandre et al., 1984). Key components modulating microtubule dynamics have been identified through studies in *Xenopus* egg extracts. These include stabilizing factors, such as XMAP215, and destabilizing factors, such as Stathmin/OP18 and XKCM1 (Belmont and Mitchison, 1996; Gard and Kirschner, 1987; Desai et al., 1999). Stabilizing and destabilizing factors are thought to oppose each other to maintain the correct steady-state length of microtubules in interphase and in metaphase (Tournebize et al., 2000). Little is known about factors that may alter microtubule dynamics during anaphase. Our results show that *zyg-8*

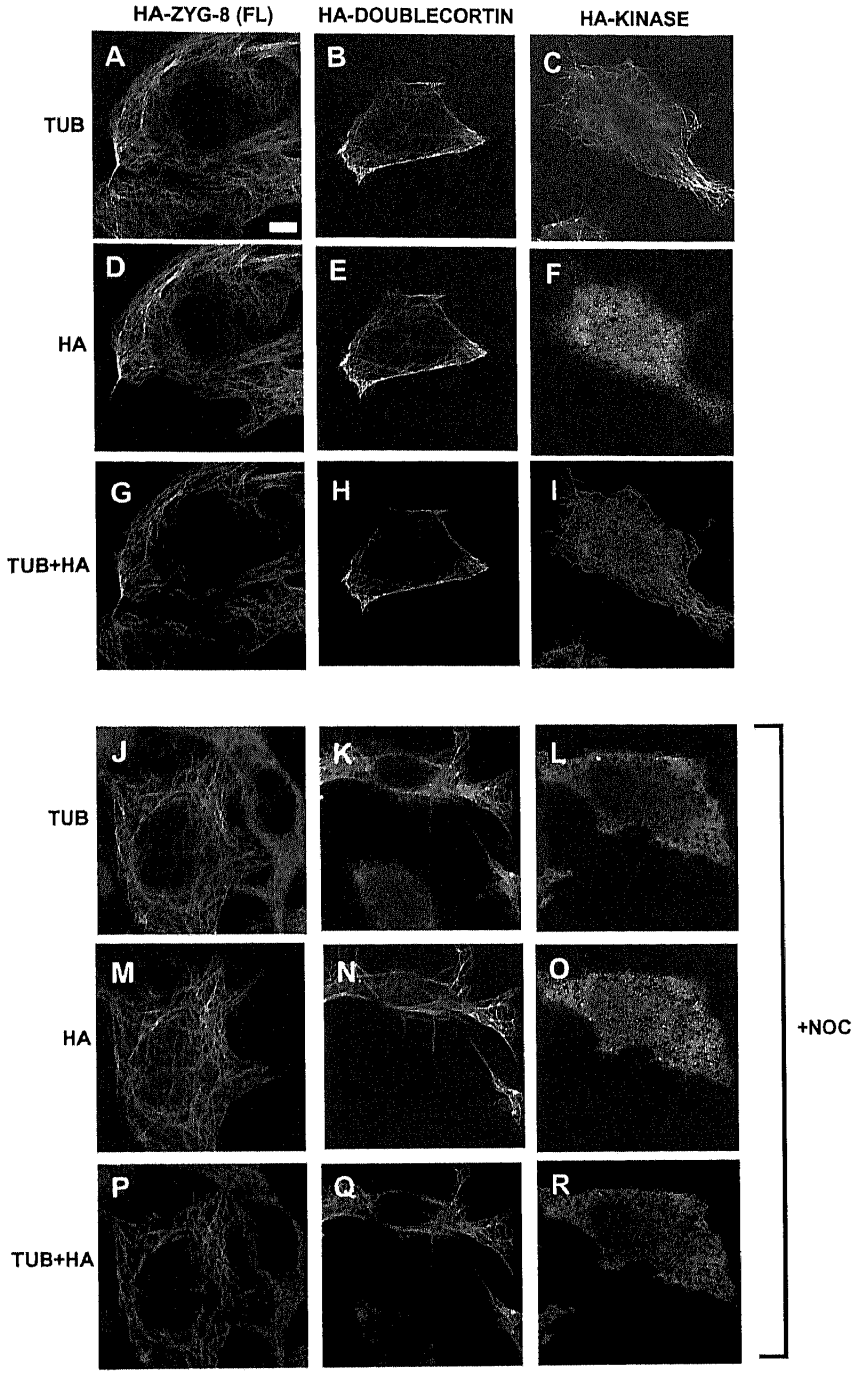

Figure 6. ZYG-8 Colocalizes with Microtubules in COS-7 Cells and Promotes Their Stability

COS-7 cells transfected with full-length HA-ZYG-8 (A, D, G, J, M, and P), the Doublecortin domain alone tagged with HA (B, E, H, K, N, and Q) or the kinase domain alone tagged with HA (C, F, I, L, O, and R) and stained with anti-tubulin (A, B, C, J, K, and L) or anti-HA (D, E, F, M, N, and O) antibodies. In the merged images, tubulin is shown in green, HA in red. All panels at same magnification. Bar = 10 μm. (A–I) Full-length HA-ZYG-8 and HA-Doublecortin colocalize with microtubules in COS-7 cells; HA-kinase localizes to the cytoplasm. (J–R) Nocodazole treatment. Cells expressing full-length HA-ZYG-8 or HA-Doublecortin have an extensive microtubule network, while untransfected cells and cells expressing HA-kinase have very few microtubules left following nocodazole treatment.

function is required to generate long microtubules at that stage of the cell cycle. Therefore, an attractive hypothesis is that ZYG-8 activity at anaphase tips the balance in favor of microtubule polymerization, thus allowing proper anaphase to take place.

ZYG-8 Is a Member of an Evolutionarily Conserved Family of MAPs

ZYG-8 is a member of a family of proteins containing a Doublecortin domain, either singly or in combination with a kinase domain. The founding member of this family, human Doublecortin (DCX), harbors only a Doublecortin domain. DCX is distributed along microtubules in cultured cortical neurons and stimulates microtubule polymerization in vitro (Francis et al., 1999; Gleeson et al., 1999; Horesh et al., 1999). In addition, missense mutations in the Doublecortin domain found in some patients with X-linked lissencephaly and double-cortex syndrome disrupt DCX microtubule binding and polymerization activities, further indicating that the Doublecortin domain confers MAP activity to DCX (Sapir et al., 2000; Taylor et al., 2000).

Like DCX, ZYG-8 promotes microtubule assembly most likely by direct interaction with the polymer. Indeed, ZYG-8 binds to microtubules in vitro and colocalizes with microtubules in *C. elegans* embryos as well as in COS-7 cells. We found that the Doublecortin domain is necessary and sufficient for colocalization of ZYG-8 with microtubules in COS-7 cells. Moreover, four *zyg-8* alleles have point mutations in conserved residues in the Doublecortin domain, including one that is altered in human patients. When expressed in COS-7 cells, the

corresponding proteins fail to colocalize with microtubules. Importantly, these findings taken together demonstrate that the function of the Doublecortin domain in promoting microtubule binding and assembly has been conserved across metazoan evolution.

ZYG-8 has a mammalian ortholog that also harbors a Doublecortin domain and a kinase domain (hereafter referred to as DCLK; Matsumoto et al., 1999; Omori et al., 1998; Sossey-Alaoui and Srivastava, 1999). DCLK is expressed primarily in the developing central nervous system and can also bind microtubules in vitro and in vivo (Burgess et al., 1999; Mizuguchi et al., 1999; Burgess and Reiner, 2000; Lin et al., 2000). While the requirement for DCLK function has not yet been tested in the animal, our data raise the possibility that DCLK, like ZYG-8, may promote microtubule assembly during anaphase, perhaps in dividing neuroblasts.

Kinase Activity Is Essential for Efficient ZYG-8 Function

Although the sequence of the kinase domain in ZYG-8 resembles that of CaM kinases, two observations suggest that calcium/calmodulin (Ca/CaM) does not regulate ZYG-8. First, ZYG-8 does not contain an apparent Ca/CaM binding site. Bona fide CaM Kinases are autoinhibited by a short region located C-terminal of the last kinase subdomain until Ca/CaM binding to this region triggers kinase activation (reviewed in Chin and Means, 2000). The region C-terminal of the last kinase subdomain in ZYG-8 is very divergent from that found in bona fide CaM kinases. In particular, a critical hydrophobic residue that mediates contact with CaM is absent from ZYG-8, as it is from DCLK. Second, the kinase activity of CPG16, a splice variant of DCLK that contains only the kinase domain, is not affected by changes in Ca/CaM levels (Silverman et al., 1999). Instead, CPG16 kinase activity is stimulated by cAMP and PKA, raising the possibility that ZYG-8 and DCLK may be regulated in a similar manner.

Recent studies of DCLK have suggested that kinase activity does not regulate microtubule binding, as "kinase dead" DCLK still binds microtubules in vitro and colocalizes with microtubules in COS-7 cells (Burgess and Reiner, 2000; Lin et al., 2000). Similarly, "kinase dead" ZYG-8 colocalizes with microtubules in COS-7 cells (J.-M.B., unpublished data). In apparent contrast to these observations, however, our findings in *C. elegans* indicate that kinase activity is required for efficient ZYG-8 function. Indeed, four *zyg-8* alleles that are predicted to lack kinase activity have a phenotype at 25°C similar to that of other *zyg-8* alleles. Therefore, kinase activity likely regulates the ability of ZYG-8 to promote microtubule assembly, perhaps through phosphorylation of the Doublecortin domain. However, the phenotype of these alleles is weaker at 16°C (P.G., unpublished data), indicating that the kinase domain contributes to, rather than being essential for, ZYG-8 function. This may explain why a difference in microtubule binding is not detected with "kinase dead" variants in COS-7 cells where proteins are overexpressed.

Microtubules and Anaphase Spindle Positioning in One-Cell Stage *C. elegans* Embryos

The mechanisms by which overall cell polarity is communicated to the cytoskeleton to achieve accurate spindle positioning are poorly understood. Our work reveals that microtubule destabilization during anaphase of one-cell stage *C. elegans* embryos results in exaggerated posterior-directed spindle movement. Why should global destabilization of microtubules result in such polar movement? We have shown that extra-spindle pulling forces dictate spindle position along the AP axis during anaphase in wild-type (Grill et al., 2001). Importantly, forces acting on the posterior spindle pole are more extensive than those acting on the anterior one, thus explaining the slight posterior spindle displacement.

As the mechanistic basis for these forces remains to be determined, we can only speculate about why they may be differentially altered following global microtubule destabilization. One possibility is that microtubule destabilization affects pulling forces differentially at the anterior and the posterior. For instance, pulling forces on the anterior may normally require anchoring of microtubules to the cortex; if this were the case, these forces would be impaired when microtubules are destabilized. In contrast, pulling forces on the posterior may normally be coupled to microtubule depolymerization; if this were the case, these forces could be enhanced when microtubules are destabilized. *zyg-8* mutant embryos will be instrumental for testing these and other models and thus increase understanding of the mechanisms that ensure precise spindle positioning during asymmetric cell division.

Experimental Procedures

C. elegans Strains

C. elegans culture was according to standard methods (Brenner, 1974). Strains carrying the following mutations and deficiency were used: *unc-32(e189); qC1 dpy-19(e1259ts) glp-1(q339); him-3(e1147); him-5(e1490); par-1(b274)* (Kemphues et al., 1988); *par-3(it71)* (Cheng et al., 1995); *zyg-8(b235ts)* (Wood et al., 1980); *zyg-8(t1518), zyg-8(t1540), zyg-8(t1547), zyg-8(t1583), zyg-8(t1608), zyg-8(t1650), zyg-8(t1681),* and *tDf5* (H. Schnabel and R. Schnabel, personal communication; Gönczy et al., 1999); *zyg-8(or450ts), zyg-8(or478ts), zyg-8(or484ts), zyg-8(or490ts), zyg-8(or535ts)* (Encalada et al., 2000); *zyg-9 (it3)* (Kemphues et al., 1986). In the course of this work, we found that *apo-1* (Gönczy et al., 1999) is allelic to *zyg-8*; the two *apo-1* alleles have been renamed *zyg-8(t1441)* and *zyg-8(t1638)*. All nonconditional *zyg-8* alleles were linked to *unc-32(e189)* and balanced by *qC1*. We tested whether *zyg-8(t1650)* or *zyg-8(b235)* were paternally rescued and found this not to be the case (data not shown).

par-3(it71) zyg-8(t1650) double mutants were generated by conventional genetic crosses. *par-2* or *par-1* function were abolished by RNAi in homozygous *zyg-8(t1650)* mutant animals. pBS-par-2 and ZC22 (Guo and Kemphues, 1995; both gifts from the Kemphues laboratory) were used as templates to generate sense and antisense RNAs (Ambion), which were then annealed to generate double-stranded RNA (*par-1*) or used as such (*par-2*). RNAi was effective because injection of wild-type animals yielded progeny with *par-2* and *par-1* phenotypes.

Spindle Positioning Defects

Animals were grown at 16°C, transferred as L4s to fresh plates, and left at 25°C for >12 hr. Gravid hermaphrodites were dissected and embryos analyzed by time-lapse DIC microscopy as described (Gönczy et al., 1999). The position of each aster was determined throughout mitosis (~4 min), as was the position of the spindle at the end of mitosis (defined by cleavage furrow ingression).

Thirteen out of fifteen *zyg-8* alleles (*b235ts*, *t1441*, *t1518*, *t1540*, *t1547*, *t1583*, *t1638*, *t1650*, *or450ts*, *or478ts*, *or484ts*, *or490ts*, *or535ts)* displayed similar spindle positioning defects. In *zyg-8(t1608)*, embryos lost structural integrity upon dissection or mounting on the agarose pad; in utero recordings revealed no other phenotypes. In *zyg-8(t1681)*, embryos failed to assemble a spindle; this is likely due to a linked mutation in another locus, since the progeny of animals transheterozygote for *zyg-8(t1681)* and *zyg-8(t1650)* assembled a normal spindle and displayed canonical spindle positioning defects.

Anti-ZYG-8 and Anti-PAR-1 Antibodies

ZYG-8

A fusion between glutathione-S-transferase (GST) and aa 458–802 in ZYG-8 was injected into rabbits according to standard procedures. Anti-GST antibodies were removed by passage through a Hitrap NHS (Pharmacia) column coupled to *E. coli* expressing GST. Anti-ZYG-8 antibodies were affinity-purified using a Hitrap NHS column coupled to the fusion protein and stored at 0.6 mg/ml. These antibodies recognize a band of ~85 kDa on Western blots of total worm extract, the expected size of ZYG-8, as well as other bands whose nature is unclear. In embryos, in addition to epitopes specific to ZYG-8 (see Figure 5), these antibodies recognize other epitopes on the nucleus and at the cortex.

PAR-1

A fusion between GST and a C-terminal fragment of PAR-1 (aa 780–1232, derived from λZAPII phage yk42e4, a gift from Y. Kohara) was expressed, purified and injected as above. Anti-PAR-1 antibodies were purified in a similar manner as above against GST and with the fusion protein, and stored at 0.87 mg/ml. The staining pattern in early embryos was similar to that obtained with other anti-PAR-1 antibodies (Guo and Kemphues, 1995). In addition, centrosomes were labeled. This aspect of the staining pattern reflects PAR-1 distribution because it is absent in *par-1(b274)* mutant embryos.

Indirect Immunofluorescence

Homozygous mutant animals were left at 25°C for >12 hr prior to dissection and fixation of embryos as described (Gönczy et al., 1999). Primary antibodies were 1:1000 mouse anti-tubulin (DM1A, Sigma); 1:1000 rabbit anti-ZYG-8; 1:3000 rabbit anti-PAR-1; 1:300 rabbit anti-PAR-2 (Pichler et al., 2000); 1:10 rabbit anti-PAR-3 (Etemad-Moghadam et al., 1995) or 1:300 rabbit anti-PAR-3 (Pichler et al., 2000); 1:4 mouse anti-P granules monoclonal supernatant (OIC14, Developmental Studies Hybridoma Bank); 1:5000 rabbit anti-PGL-1 (Kawasaki et al., 1998); 1:3000 rabbit anti-ZYG-9 (raised against a C-terminal peptide; affinity purified; 0.7 mg/ml); 1:200 rabbit anti-HA (Y11, Santa Cruz). Secondary antibodies were 1:1000 goat anti-mouse Alexa-488 (Molecular Probes) and 1:1000 donkey anti-rabbit Cy3 (Dianova). Slides were counterstained with Hoechst 33258 (Sigma) to reveal DNA. Indirect immunofluorescence was imaged on an LSM510 Zeiss confocal microscope. Optical slices for embryos were 1.0–1.2 μm thick; the stage was refocused slightly between channels in some cases. Images were processed with Adobe Photoshop.

Polarity Markers

Distribution of PAR proteins and P granules was determined between early pronuclear migration and late anaphase. AP polarity was ascertained usually by the position of the polar bodies, which in general mark the embryo anterior (Goldstein and Hird, 1996). Embryos with laterally located polar bodies were not analyzed because their polarity could not be unambiguously determined.

Length Measurements

Five wild-type and *zyg-8(t1650)* mutant (before exaggerated displacement) anaphase embryos stained with anti-tubulin antibodies were analyzed. The three longest astral microtubules projecting toward the anterior cortex were identified in each embryo and imaged. The length of each astral microtubule, as well as the distance separating it from the cortex, were determined using the public domain NIH image program 1.62b7 (developed at the U.S. National Institutes of Health and available at http://rsb.info.nih.gov/nih-image/). Embryos between metaphase and late anaphase stained with anti-ZYG-9 antibodies were analyzed similarly to measure the distance between the two spindle poles.

Nocodazole Treatment

Two protocols were used to subject wild-type one-cell stage embryos (n = 34) undergoing centration/rotation to nocodazole. In most cases, pronuclear migration was observed in a watch glass containing M9 (Brenner, 1974), and individual embryos transferred upon pronuclear meeting to a 2% or 4% agarose pad. The medium was replaced 60–90 s later by M9 containing 100 μg/ml (33 μM) nocodazole (Sigma). In some cases, embryos were transferred in bulk to the agarose pad, the medium exchanged with that containing nocodazole, and embryos undergoing centration/rotation selected for analysis. A coverslip was placed on the agarose pad and tapped gently with forceps to damage the eggshell and render it permeable to nocodazole.

The 34 embryos fell into three groups. In one group (n = 16), there was no apparent effect on the first cell division, probably because of insufficient exposure to nocodazole. In the second group (n = 3), centration/rotation did not take place and the spindle was barely visible, presumably because of excess exposure to nocodazole. In the third group (n = 15), centration/rotation took place, in general like in wild-type, but the spindle was smaller as a result of nocodazole treatment. The spindle drifted to the posterior during anaphase in 14/15 embryos and toward the anterior in 1/5 embryos.

Characterization of the *zyg-8* Gene and Sequencing of Mutant Alleles

RNAi against Y79H2A.11 (nt 59685–60671 and 61789–62840 on YAC Y79H2A) and Y75B8A.36 (nt 255–800 on YAC Y75B8A) resulted in a *zyg-8* like phenotype. Inserts in corresponding λZAPII phages yk54f7 and yk420b3 (gifts from Yuji Kohara) were sequenced, confirming that Y79H2A.11 and Y75B8A.36 represent a single gene. To obtain full-length *zyg-8* mixed developmental stages worms were used for RT-PCR; the resulting PCR product was sequenced, found to be in agreement with the genome sequence and joined with yk420b3 using a unique NcoI restriction site, generating full-length *zyg-8* (accession no. AJ319870).

For sequencing of alleles *t1518*, *t1547*, and *t1650*, primer pairs were designed to amplify each of the 10 exons and all exon/intron boundaries. Genomic DNA was prepared from homozygous mutant animals, the relevant pieces of DNA amplified by PCR and sequenced (MWG Biotech). For sequencing of the remaining alleles, cDNAs were prepared with the RNeasy and One-step RT-PCR kit (Qiagen) and sequenced (ISREC core facility; Microsynth). All mutations described in the text have been found in two independent preparations and sequencing reactions. No mutations were found in the coding sequence of *zyg-8(b235)* or *zyg-8(t1608)*.

GFP::ZYG-8

Full-length *zyg-8* was cloned into the pie-1/GFP expression vector (Reese et al., 2000). GFP::ZYG-8 (1 ng/ml) mixed with 1 ng/ml transformation marker *rol-6* (pRF4) linearized with EcoRI (Mello et al., 1991) and 60 ng/ml wild-type genomic DNA linearized with PvuII (Kelly et al., 1997) was injected into *zyg-8(t1650) unc-32(e189)/qC1* heterozygous animals that were left at 25°C. Heterozygous F1 rolling animals were singled and resulting F2 animals tested. 18/28 F2 Unc Rol animals (from four independent lines) gave rise to >50 progeny; 0/20 F2 Unc non Rol control animals gave rise to any progeny. A similar protocol was followed for *zyg-8(b235ts)*, except that injected animals and their F1 progeny initially spent 24 hr at 20°C. Nine out of twenty-seven F2 Rol animals gave rise to >50 progeny; 0/24 F2 non Rol control animals gave rise to >10 progeny (as in the original strain). GFP::ZYG-8 expressing embryos were analyzed using dual time-lapse DIC and fluorescence spinning disc confocal microscopy as described (Oegema et al., 2001).

Microtubules Copelleting Assays

Taxol-stabilized microtubules were prepared from bovine brain-purified tubulin essentially as described (Hyman et al., 1991). [^{35}S]methionine ZYG-8 was produced using the TNT T7 Quick for

PCR DNA kit (Promega). Copelleting assays were performed essentially as described (Spittle et al., 2000) with the following modifications: (1) PEM was substituted by BRB80 (80 mM PIPES, 1 mM $MgCl_2$, 1 mM EGTA [pH 6.8]); (2) [^{35}S]methionine ZYG-8 was precleared twice at 55,000 rpm for 30 min in a TLA 100.2 rotor; (3) 5 μl of clarified ZYG-8 lysate was incubated with taxol-stabilized microtubules for 20 min at 37°C in the presence of 1 mM GTP, 20 mM taxol, and 10 mg/mL BSA; (4) samples were pelleted through a 50% glycerol cushion for 10 min at 50,000 rpm in a TLA 100.2 rotor and the soluble and insoluble fractions prepared for SDS-PAGE/autoradiography and densitometry analysis.

Cell Culture and Transfection Experiments

COS-7 cells were grown on glass coverslips to 60% confluency in DMEM supplemented with 10% fetal calf serum. Cells were transfected using the DEAE-dextran method (Sambrook and Russell, 2001) with cDNAs encoding full-length ZYG-8 (aa 1–802), the Doublecortin domain alone (aa 1–464), or the kinase domain alone (aa 477–802) inserted into pHA-L11 Tag (a gift from S. Schmidt, based on pEGFP-C2a, Clontech). After 36 hr, methanol fixation/permeabilization and immunofluorescence were performed as described by A. Desai (http://iccbweb.med.harvard.edu/mitchisonlab/Pages/gen1.html). When needed, cells were left 30 min prior to fixation in 10 μm nocodazole or on ice.

Acknowledgments

We are grateful to Heinke Schnabel and Ralf Schnabel for having made *zyg-8* mutant alleles available to us. We thank Arshad Desai for advice on microtubule copelleting assays, and Ken Kemphues, Yuji Kohara, Susanne Schmidt, Geraldine Seydoux, and Susan Strome for precious reagents. Some strains were obtained from the *Caenorhabditis* Genetics Center, which is funded by the NIH National Center for Research Resources (NCRR). For help in improving the manuscript, we thank Arshad Desai, Anne Ephrussi, Stephan Grill, Matthias Peter, Heinke Schnabel, and Ralf Schnabel. P.G. was a fellow from the Human Frontier Science Program (LT-202/96) and the Swiss National Science Foundation (TMR 83EU-045376) during parts of this project. J.-M.B. is supported by a fellowship from the Association pour la Recherche contre le Cancer (A00/4). Work in the Hyman laboratory is supported by the Max Planck Society, work in the Gönczy laboratory by the Swiss National Science Foundation.

Received October 30, 2000; revised July 31, 2001.

References

Albertson, D. (1984). Formation of the first cleavage spindle in nematode embryos. Dev. Biol. *101*, 61–72.

Belmont, L.D., and Mitchison, T.J. (1996). Identification of a protein that interacts with tubulin dimers and increases the catastrophe rate of microtubules. Cell *84*, 623–631.

Boyd, L., Guo, S., Levitan, D., Stinchcomb, D.T., and Kemphues, K.J. (1996). PAR-2 is asymmetrically distributed and promotes association of P granules and PAR-1 with the cortex in *C. elegans* embryos. Development *122*, 3075–3084.

Brenner, S. (1974). The genetics of *Caenorhabditis elegans*. Genetics *77*, 71–94.

Burgess, H.A., and Reiner, O. (2000). Doublecortin-like kinase is associated with microtubules in neuronal growth cones. Mol. Cell. Neurosci. *16*, 529–541.

Burgess, H.A., Martinez, S., and Reiner, O. (1999). KIAA0369, doublecortin-like kinase, is expressed during brain development. J. Neurosci. Res. *58*, 567–575.

Cheng, N.N., Kirby, C.M., and Kemphues, K.J. (1995). Control of cleavage spindle orientation in Caenorhabditis elegans: the role of the genes par-2 and par-3. Genetics *139*, 549–559.

Chin, D., and Means, A.R. (2000). Calmodulin: a prototypical calcium sensor. Trends Cell Biol. *10*, 322–328.

des Portes, V., Pinard, J.M., Billuart, P., Vinet, M.C., Koulakoff, A., Carrie, A., Gelot, A., Dupuis, E., Motte, J., Berwald-Netter, Y., Catala, M., Kahn, A., Beldjord, C., and Chelly, J. (1998). A novel CNS gene required for neuronal migration and involved in X-linked subcortical laminar heterotopia and lissencephaly syndrome. Cell *92*, 51–61.

Desai, A., and Mitchison, T.J. (1997). Microtubule polymerization dynamics. Annu. Rev. Cell Dev. Biol. *13*, 83–117.

Desai, A., Verma, S., Mitchison, T.J., and Walczak, C.E. (1999). Kin I kinesins are microtubule-destabilizing enzymes. Cell *96*, 69–78.

Encalada, S.E., Martin, P.R., Phillips, J.B., Lyczak, R., Hamill, D.R., Swan, K.A., and Bowerman, B. (2000). DNA replication defects delay cell division and disrupt cell polarity in early Caenorhabditis elegans embryos. Dev. Biol. *228*, 225–238.

Etemad-Moghadam, B., Guo, S., and Kemphues, K.J. (1995). Asymmetrically distributed PAR-3 protein contributes to cell polarity and spindle alignement in early *C. elegans* embryos. Cell *83*, 743–752.

Francis, F., Koulakoff, A., Boucher, D., Chafey, P., Schaar, B., Vinet, M.C., Friocourt, G., McDonnell, N., Reiner, O., Kahn, A., et al. (1999). Doublecortin is a developmentally regulated, microtubule-associated protein expressed in migrating and differentiating neurons. Neuron *23*, 247–256.

Gard, D.L., and Kirschner, M.W. (1987). A microtubule-associated protein from *Xenopus* eggs that specifically promotes assembly at the plus-end. J. Cell Biol. *105*, 2203–2215.

Gleeson, J.G., Allen, K.M., Fox, J.W., Lamperti, E.D., Berkovic, S., Scheffer, I., Cooper, E.C., Dobyns, W.B., Minnerath, S.R., Ross, M.E., and Walsh, C.A. (1998). Doublecortin, a brain-specific gene mutated in human X-linked lissencephaly and double cortex syndrome, encodes a putative signaling protein. Cell *92*, 63–72.

Gleeson, J.G., Lin, P.T., Flanagan, L.A., and Walsh, C.A. (1999). Doublecortin is a microtubule-associated protein and is expressed widely by migrating neurons. Neuron *23*, 257–271.

Goldstein, B., and Hird, S.N. (1996). Specification of the anteroposterior axis in *Caenorhabditis elegans*. Development *122*, 1467–1474.

Gönczy, P., Schnabel, H., Kaletta, T., Amores, A.D., Hyman, T., and Schnabel, R. (1999). Dissection of cell division processes in the one cell stage *Caenorhabditis elegans* embryo by mutational analysis. J. Cell Biol. *144*, 927–946.

Gönczy, P., Echeverri, C., Oegema, K., Coulson, A., Jones, S.J.M., Copley, R.R., Duperon, J., Oegema, J., Brehm, M., Cassin, E., et al. (2000). Functional genomic analysis of cell division in *C. elegans* using RNAi of genes on chromosome III. Nature *408*, 331–336.

Grill, S.W., Gönczy, P., Stelzer, E.H., and Hyman, A.A. (2001). Polarity controls forces governing asymmetric spindle positioning in the *Caenorhabditis elegans* embryo. Nature *409*, 630–633.

Guo, S., and Kemphues, K.J. (1995). *par-1*, a gene required for establishing polarity in *C. elegans* embryos, encodes a putative Ser/Thr kinase that is asymmetrically distributed. Cell *81*, 611–620.

Hanks, S.K., and Hunter, T. (1995). The eukaryotic protein kinase superfamily: kinase (catalytic) domain structure and classification. FASEB J. *9*, 576–596.

Horesh, D., Sapir, T., Francis, F., Wolf, S.G., Caspi, M., Elbaum, M., Chelly, J., and Reiner, O. (1999). Doublecortin, a stabilizer of microtubules. Hum. Mol. Genet. *8*, 1599–1610.

Hung, T.J., and Kemphues, K.J. (1999). PAR-6 is a conserved PDZ domain-containing protein that colocalizes with PAR-3 in *Caenorhabditis elegans* embryos. Development *126*, 127–135.

Hyman, A.A., and White, J.G. (1987). Determination of cell division axes in the early embryogenesis of *Caenorhabditis elegans*. J. Cell Biol. *105*, 2123–2135.

Hyman, A., Drechsel, D., Kellogg, D., Salser, S., Sawin, K., Steffen, P., Wordeman, L., and Mitchison, T. (1991). Preparation of modified tubulins. Methods Enzymol. *196*, 478–485.

Kaltschmidt, J.A., Davidson, C.M., Brown, N.H., and Brand, A.H. (2000). Rotation and asymmetry of the mitotic spindle direct asymmetric cell division in the developing central nervous system. Nat. Cell Biol. *2*, 7–12.

Kawasaki, I., Shim, Y.H., Kirchner, J., Kaminker, J., Wood, W.B., and Strome, S. (1998). PGL-1, a predicted RNA-binding component of germ granules, is essential for fertility in C. elegans. Cell *94*, 635–645.

Kelly, W.G., Xu, S., Montgomery, M.K., and Fire, A. (1997). Distinct

requirements for somatic and germline expression of a generally expressed Caernorhabditis elegans gene. Genetics *146*, 227–238.

Kemphues, K.J., and Strome, S. (1997). Fertilization and establishment of polarity in the embryo. In *C. elegans* II, D.L. Riddle, T. Blumenthal, B.J. Meyer, and J.R. Priess, eds. (Cold Spring Harbor, NY: Cold Spring Harbor Laboratory Press), pp. 335–359.

Kemphues, K.J., Kusch, M., and Wolf, N. (1988). Maternal-effect lethal mutations on linkage group II of *Caenorhabditis elegans*. Genetics *120*, 977–986.

Kemphues, K.J., Priess, J.R., Morton, D.G., and Cheng, N. (1988). Identification of genes required for cytoplasmic localization in early *C. elegans* embryos. Cell *52*, 311–320.

Kemphues, K.J., Wolf, N., Wood, W.B., and Hirsh, D. (1986). Two loci required for cytoplasmic organization in early embryos of *Caenorhabditis elegans*. Dev. Biol. *113*, 449–460.

Knoblich, J.A., Jan, L.Y., and Jan, Y.N. (1995). Asymmetric segregation of Numb and Prospero during cell division. Nature *377*, 624–627.

Korinek, W.S., Copeland, M.J., Chaudhuri, A., and Chant, J. (2000). Molecular linkage underlying microtubule orientation toward cortical sites in yeast. Science *287*, 2257–2259.

Lee, L., Tirnauer, J.S., Li, J., Schuyler, S.C., Liu, J.Y., and Pellman, D. (2000). Positioning of the mitotic spindle by a cortical-microtubule capture mechanism. Science *287*, 2260–2262.

Lin, P.T., Gleeson, J.G., Corbo, J.C., Flanagan, L., and Walsh, C.A. (2000). DCAMKL1 encodes a protein kinase with homology to doublecortin that regulates microtubule polymerization. J. Neurosci. *20*, 9152–9161.

Matsumoto, N., Pilz, D.T., and Ledbetter, D.H. (1999). Genomic structure, chromosomal mapping, and expression pattern of human DCAMKL1 (KIAA0369), a homologue of DCX (XLIS). Genomics *56*, 179–183.

Matthews, L.R., Carter, P., Thierry-Mieg, D., and Kemphues, K. (1998). ZYG-9, a *Caenorhabditis elegans* protein required for microtubule organization and function, is a component of meiotic and mitotic spindle poles. J. Cell Biol. *141*, 1159–1168.

Mello, C.C., Kramer, J.M., Stinchcomb, D., and Ambros, V. (1991). Efficient gene transfer in C. elegans: extrachromosomal maintenance and integration of transforming sequences. EMBO J. *10*, 3959–3970.

Miller, R.K., Cheng, S.C., and Rose, M.D. (2000). Bim1p/Yeb1p mediates the Kar9p-dependent cortical attachment of cytoplasmic microtubules. Mol. Biol. Cell *11*, 2949–2959.

Mizuguchi, M., Qin, J., Yamada, M., Ikeda, K., and Takashima, S. (1999). High expression of doublecortin and KIAA0369 protein in fetal brain suggests their specific role in neuronal migration. Am. J. Pathol. *155*, 1713–1721.

Oegema, K., Desai, A., Rybina, S., Kirkham, M., and Hyman A.A. (2001). Functional analysis of kinetochore assembly in *C. elegans*. J. Cell Biol. *153*, 1209–1226.

Omori, Y., Suzuki, M., Ozaki, K., Harada, Y., Nakamura, Y., Takahashi, E., and Fujiwara, T. (1998). Expression and chromosomal localization of KIAA0369, a putative kinase structurally related to Doublecortin. J. Hum. Genet. *43*, 169–177.

Palmer, R.E., Sullivan, D.S., Huffaker, T., and Koshland, D. (1992). Role of astral microtubules and actin in spindle orientation and migration in the budding yeast Saccharomyces cerevisiae. J. Cell Biol. *119*, 583–593.

Picciotto, M.R., Czernik, A.J., and Nairn, A.C. (1993). Calcium/calmodulin-dependent protein kinase I. cDNA cloning and identification of autophosphorylation site. J. Biol. Chem. *268*, 26512–26521.

Pichler, S., Gönczy, P., Schnabel, H., Pozniakowski, A., Ashford, A., Schnabel, R., and Hyman, A.A. (2000). OOC-3, a novel putative transmembrane protein required for establishment of cortical domains and spindle orientation in the P_1 blastomere of *C. elegans embryos*. Development *127*, 2063–2073.

Rappaport, R. (1971). Cytokinesis in animal cells. Int. Rev. Cytol. *31*, 169–213.

Reese, K.J., Dunn, M.A., Waddle, J.A., and Seydoux, G. (2000). Asymmetric segregation of PIE-1 in C. elegans is mediated by two complementary mechanisms that act through separate PIE-1 protein domains. Mol. Cell *6*, 445–455.

Sambrook, J., and Russell, D.W. (2001). Molecular Cloning (Cold Spring Harbor, NY: Cold Spring Harbor Laboratory Press).

Sapir, T., Horesh, D., Caspi, M., Atlas, R., Burgess, H.A., Wolf, S.G., Francis, F., Chelly, J., Elbaum, M., Pietrokovski, S., and Reiner, O. (2000). Doublecortin mutations cluster in evolutionarily conserved functional domains. Hum. Mol. Genet. *9*, 703–712.

Silverman, M.A., Benard, O., Jaaro, H., Rattner, A., Citri, Y., and Seger, R. (1999). CPG16, a novel protein serine/threonine kinase downstream of cAMP-dependent protein kinase. J. Biol. Chem. *274*, 2631–2636.

Sossey-Alaoui, K., and Srivastava, A.K. (1999). DCAMKL1, a brain-specific transmembrane protein on 13q12.3 that is similar to doublecortin (DCX). Genomics *56*, 121–126.

Spittle, C., Charrasse, S., Larroque, C., and Cassimeris, L. (2000). The interaction of TOGp with microtubules and tubulin. J. Biol. Chem. *275*, 20748–20753.

Tabuse, Y., Izumi, Y., Piano, F., Kemphues, K.J., Miwa, J., and Ohno, S. (1998). Atypical protein kinase C cooperates with PAR-3 to establish embryonic polarity in *Caenorhabditis elegans*. Development *125*, 3607–3614.

Takemura, R., Okabe, S., Umeyama, T., Kanai, Y., Cowan, N.J., and Hirokawa, N. (1992). Increased microtubule stability and alpha tubulin acetylation in cells transfected with microtubule-associated proteins MAP1B, MAP2 or tau. J. Cell Sci. *103*, 953–964.

Taylor, K.R., Holzer, A.K., Bazan, J.F., Walsh, C.A., and Gleeson, J.G. (2000). Patient mutations in doublecortin define a repeated tubulin-binding domain. J. Biol. Chem. *275*, 34442–34450.

Tournebize, R., Popov, A., Kinoshita, K., Ashford, A.J., Rybina, S., Pozniakovsky, A., Mayer, T.U., Walczak, C.E., Karsenti, E., and Hyman, A.A. (2000). Control of microtubule dynamics by the antagonistic activities of XMAP215 and XKCM1 in Xenopus egg extracts. Nat. Cell Biol. *2*, 13–19.

Vandre, D.D.P., Kronenbusch, P.J., and Borisy, G.G. (1984). Interphase-mitosis transition: microtubule rearrangements in cultured cells and sea urchin eggs. In Molecular Biology of the cytoskeleton, G.G. Borisy, D.W. Cleveland, and D.B. Murphey, eds. (Cold Spring Harbor, NY: Cold Spring Harbor Laboratory Press), pp. 3–16.

Wood, W.B., Hecht, R., Carr, S., Vanderslice, R., Wolf, N., and Hirsh, D. (1980). Parental effects and phenotypic characterization of mutations that affect early development in *Caenorhabditis elegans*. Dev. Biol. *74*, 446–469.